Monolithic optofluidic chips: from optical manipulation of single cells to quantum sensing of fluids

Roberto OSELLAME [1,2,*]

* Corresponding author: Tel.: ++39 02 2399 6075; Fax: ++39 02 2399 6126;
Email: roberto.osellame@ifn.cnr.it
1: Istituto di Fotonica e Nanotecnologie, Consiglio Nazionale delle Ricerche (CNR), Milano (Italy)
2: Dipartimento di Fisica, Politecnico di Milano, Milano (Italy)

Abstract We report on a new class of integrated optofluidic devices, fabricated by femtosecond laser micromachining. The capability to combine optical waveguides with microfluidic channels in the same glass chip provides a very powerful platform, introducing new tools in the field of optical sensing. Two recent applications that greatly benefitted from this novel technology are on-chip optical manipulation of single cells by optical forces and optical sensing of the refractive index of fluids by quantum states of light. The specific properties of robustness, alignment free and portability of these devices pave the way to the use of these advanced sensing technologies outside the lab, in a real application environment.

Keywords: Laser microfabrication, optofluidic devices, cell mechanics, quantum sensing

1. Introduction

Femtosecond lasers are powerful tools for volume microstructuring of transparent materials. Optical waveguide circuits can be directly written without any photolithographic process and exploiting unique three-dimensional capabilities in defining the circuit layout [Gattass (2008), Della Valle (2009)]. In addition, femtosecond-laser irradiation of fused silica followed by chemical etching in HF solution allows the manufacturing of directly buried microfluidic channels, due to the enhanced (by up to two orders of magnitude) etching rate of the irradiated material with respect to the pristine one. This opens the possibility of using a single femtosecond laser system for the production of optical circuits and their possible integration with a microfluidic channel network [Osellame (2007)].

This enabling technology has been exploited in such diverse fields as optical detection in lab-on-a-chip [Martinez (2009), Crespi (2010)] and integrated quantum optical circuits [Sansoni (2012), Corrielli (2013)].

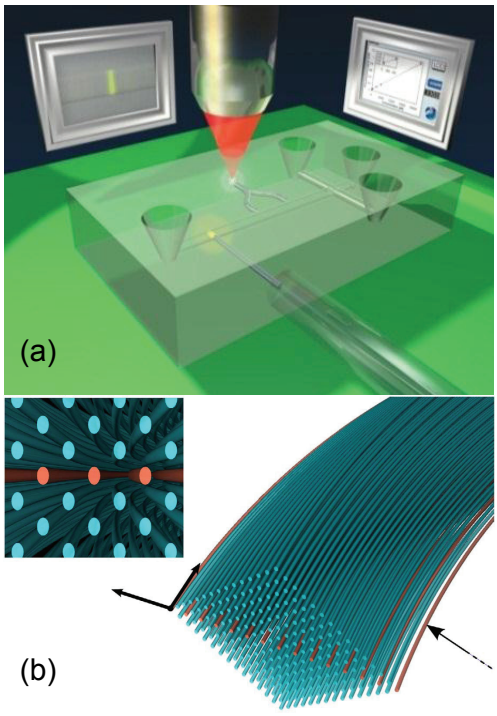

Fig. 1. a) Direct writing of optical waveguides in lab-on-a-chip devices for integrated fluorescence sensing [Martinez (2009)]. b) Two-dimensional waveguide array with tailored curvature and refractive index change to study the correlated Bloch oscillations of interacting particles [Corrielli (2013)].

In this work we present the latest application of this technological platform to two advanced sensing configuration: optical manipulation of cells to measure their mechanical properties at the single cell level; refractive index measurements on relevant liquid samples with quantum states of light to maximize the amount of information that can be retrieved from each incident photon.

2. Integrated optical manipulation of single cells

Current frontier of cellular biology is the manipulation, analysis and sorting of single cells. Populations of cells in culture and in organisms, although considered nominally identical, often present some heterogeneity that poses a severe challenge for many experimental measurements. In fact, differences among cells of the same population may unravel the complexity of many biological phenomena [de Souza (2012)]. Optical stretching is a powerful technique to study the mechanical properties of single suspended cells by means of the application of optical forces [Guck (2001)]. Single cell analysis and sorting are powerful tools for the selection of a small group of cells of interest out of a wide and heterogeneous population, such as blood samples, cells from resected tumors or in vitro cultures; the goal of such analysis being the diagnosis of pathological disorders or the separation of specific cells for further analysis.

In recent years, considerable effort has been devoted to the development of integrated and low-cost optofluidic devices able to handle single cells. Such devices usually rely on microfluidic circuits that guarantee a controlled flow of the cells with optical radiations often exploited to probe or manipulate the cells under test. Among the different microfabrication technologies, femtosecond laser micromachining (FLM) [Osellame (2011)] is ideally suited for this purpose as it provides the integration of both microfluidic and optical functions on the same glass chip leading to monolithic, perfectly aligned, robust and portable optofluidic devices.

2.1 Results and Discussion

Here we present two integrated optical devices for single cell studies, which combine microfluidic and optical tweezers technologies to implement in monolithic chips two key functionalities for cell analysis and manipulation: optical stretching and cell sorting. A schematic of the optical stretcher (OS) and fluorescence activated cell sorter (FACS) working principle implemented in our devices are shown in Fig. 1 (a) and (b), respectively.

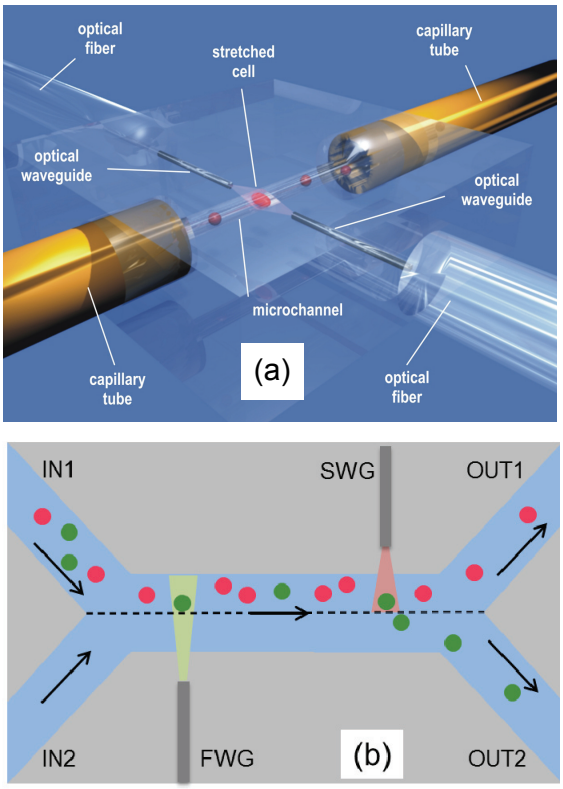

Fig. 2. Schematic diagram of the working principle for (a) the optical stretcher [Bellini (2012)], and (b) the fluorescence activated optical sorter [Bragheri (2012)].

In an OS, cells in suspension in a microfluidic channel are delivered serially into the trapping region where a dual beam laser trap (DBLT) attracts a single cell and holds it in place. By increasing the optical power emitted by the opposite waveguides, the surface forces exerted on the trapped cells are sufficient to induce a controlled and non-

destructive deformation of the cells, providing a reliable measurement of their mechanical properties.

The optical sorter design is instead based on an X-shaped channel (Fig. 1(b)) where two input channels merge in a central section, where fluorescence investigation and sorting are performed, and subsequently separating into two output channels. The sample enters from input IN1 while buffer solution enters from input IN2. By suitably balancing the pressures at the channel ends a laminar flow is achieved so that everything entering input IN1 exits from output OUT1. Sorting is achieved by applying optical forces that move the cells in the other half of the channel, thus directing it to the corresponding output. Such sorter is automatically activated on the basis of the integrated fluorescence measurement (FACS). In detail, an optical waveguide (FWG) emits laser light into the channel covering its entire section and illuminating all the cells flowing in the channel. If a cell provides a fluorescence signal, a second waveguide (SWG) emits a light beam for a short time interval synchronized with the fluorescent cell motion in order to push it to the OUT2 channel.

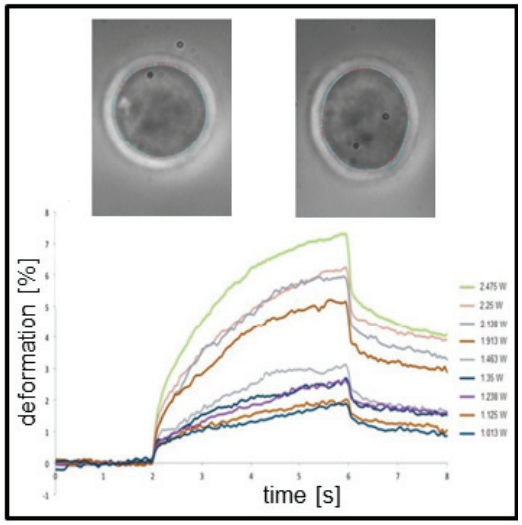

Fig. 3. Phase contrast microscope images of trapped and stretched HL60 cell in a stretching experiment (top) with automatic contour recognition. (bottom) HL60 response to a step-like applied optical stimulus for different stretching power values [Bellini (2012)].

Both devices have been fabricated through femtosecond laser micromachining. The OS is realized by waveguide inscription on a commercial microfluidic chip (Translume Inc.), whose fabrication is also based on femtosecond laser irradiation followed by chemical etching in HF. The monolithic cell sorter is completely fabricated in our lab with the same technology.

The capability of the OS and of the microFACS has been tested respectively on HL60 cells and on a cell sample constituted of human transformed fibroblasts transfected with a plasmid encoding the enhanced green fluorescent protein (EGFP). Figure 3 shows HL60 response to step-like increase in applied optical stress for different stretching optical forces. Top panels also show two phase-contrast microscope images of a cell trapped (left) and stretched (right) by the optical power emitted by the two waveguides in the DBLT [Bellini (2012)].

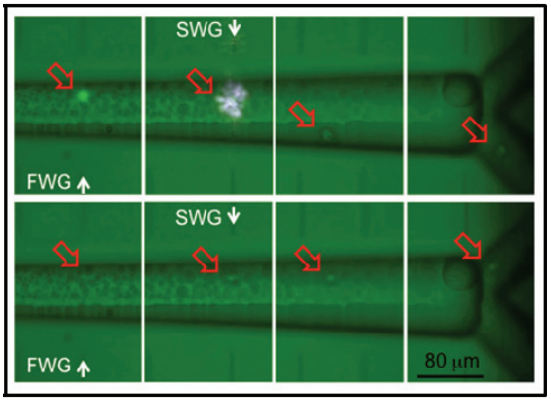

Fig. 4. Sequence of CCD frames demonstrating the sorting functionality activated by fluorescence when fluorescent (top) and non-fluorescent (bottom) cells are inserted in the optofluidic cell sorter [Bragheri (2012)].

The functionality of the fluorescence-activated cell sorter is demonstrated in Fig. 4, which shows a sequence of frames documenting the device operation when either a fluorescent (top) or a non-fluorescent cell (bottom) is flowing in the channel. To excite EGFP fluorescence we coupled into the FWG a 3 mW, 473 nm laser. When a fluorescent cell is illuminated by the radiation emitted from FWG it provides a fluorescence signal recognized by the software; after a suitable delay time (about 0.3 s) the 1070-nm laser power is raised so as to push the cell when it

crosses the region illuminated by SWG. Afterwards the cell flows in the lower half of the channel and exits from OUT2. On the other hand when a non-fluorescent cell is illuminated by the blue excitation wavelength it doesn't emit any fluorescence signal and continues to flow in the upper half of the channel [Bragheri (2012)].

3 Quantum sensing of protein concentration

Even the most advanced sensors are bound by a limit in precision—the shot noise or standard quantum limit (SQL) that arises from statistical fluctuations. In a conventional optical interferometer, for example, the precision with which an unknown optical phase ϕ can be measured is limited to $\delta\phi=N^{-1/2}$, where N is the (average) number of photons used to probe ϕ [Giovannetti (2004), Walther (2004), Mitchell (2004), Nagata (2007)]. Increasing N is usually possible, by increasing laser power for example. However, in some scenarios, the practical limits of laser power are reached and increasing the integration time will reduce the bandwidth of the measurement below that required—gravity wave interferometers are a key example [Goda (2008)]. In other scenarios, the sample to be measured may be sensitive to light, such that one would like to minimise the photon flux or total number of photons that the sample is exposed to in order to reach the required precision. In other words, one wishes to gain the maximum information allowable by the laws of physics for a given perturbation of the sample. By harnessing quantum superposition and entanglement the SQL can be overcome - quantum metrology enables the more fundamental Heisenberg limit of precision, $\delta\phi=1/N$, to be reached [Giovannetti (2004)].

Biological samples of interest are often in liquid form. To perform practical quantum metrology over real samples, the quantum optical circuits needs to be interfaced with microfluidic circuits. We use the optofluidic device shown in Fig. 5, consisting of a microfluidic channel that passes through one arm of a Mach-Zehnder interferometer (MZI), fabricated by femtosecond laser micromachining [Gattass (2008), Della Valle (2009), Crespi (2010)]. This device combines the stability of integrated optics for high visibility quantum and classical interference [Politi (2008), Sansoni (2010)] with high precision handling of fluid samples [Osellame (2011), Whitesides (2006)].

When a solution is fed into the microfluidic channel, any relative phase shift of light (and thereby concentration-dependent refractive index) in the sensing arm with respect to that acquired in the reference arm can be estimated from the interference fringes.

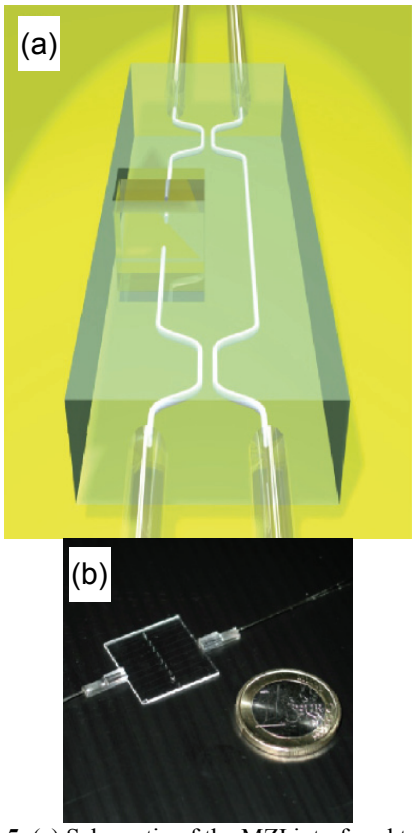

Fig. 5. (a) Schematic of the MZI interfaced to the microchannel. The fluidic channel has a rectangular cross-section of 500 μm×55 μm and extends from the top to the bottom surface of the glass substrate (~1mm thickness). The MZI consists of two 50:50 directional couplers and has two arms of equal geometrical length; one waveguide crosses perpendicular to the microchannel, while the other passes externally. (b) Picture of the device, with several interferometers and microchannels on chip, together with the fiber arrays for coupling input and output light [Crespi (2012)].

The period of the interference fringes and the measurement precision $\delta\phi$ depend on the

particular state of light used to probe the sample. To achieve the Heisenberg limit of precision, the canonical example of quantum state is the NOON state (i.e., a superposition between the situation with N photons in the sensing arm of the MZI and 0 in the reference arm, and the situation with 0 photons in the sensing arm and N photons in the reference arm), which can achieve super-sensitivity and super-resolution [Giovannetti (2004), Walther (2004), Mitchell (2004), Nagata (2007)]. The latter results in a fringe periodicity that is 1/N times shorter than the one obtained with classical light. We test the operation of our device for the N=2 NOON state, which enables supersensitity and super-resolution, and can be generated from two single photons input into a directional coupler [Rarity (1990)].

3.1 Results and Discussion

The device was fabricated by femtosecond laser micromachining in a fused-silica sample to enable the integration of optical waveguides and microfluidic channels in a three-dimensional architecture [Osellame (2011)].

Photon pairs at λ = 785 nm were generated via spontaneous parametric down-conversion (SPDC) in a nonlinear crystal [Crespi (2012)] and collected into polarization maintaining fibers. The photon pairs were then coupled into the MZI via fiber arrays.

To test the operation of our device with a real sample, we chose bovine serum albumin (BSA) in aqueous buffer solutions as a model fluidic sample that is stable and well characterized [Peters (1975)]. We performed sensing measurements using one photon and two photon inputs for 15 different concentrations of BSA ranging from 0% to 7% in 0.5% steps. Cleaning of the microchannel with deionized water and acetone was performed before and after each measurement.

The single-photon fringe is obtained by coupling only one photon from the SPDC pair into the MZI and counting the number of detections from one output of the MZI. Figure 6(a) shows the single photon count rate normalized with respect to the sum of the singles from the two outputs together [Crespi (2012)]. A visibility V_1 = 94±2.2% is estimated from the fit, compared to a theoretical prediction V_1^{th} = 97%, calculated taking into account the device losses.

Two-photon fringes were measured by coupling photon pairs into the two input waveguides of the MZI and detecting coincidences from the two separate output channels. Coincidence events are normalized with respect to the sum of all the possible two-photon outputs [Crespi (2012)], and shown in Fig. 6(b) together with the theoretical fit function. As expected, the period is half that of the single photon fringe due to super-resolution. The visibility of the fit is V_2 = 82±4.8%, in agreement with the theoretical prediction for the interferometer including losses V_2^{th} = 88%. This value exceeds the threshold for supersensitivity [Resch (2007)]: V_2^{SQL} = 70.7%. Nevertheless, this value does not include source and detector efficiencies which prevent current experiments to beat the standard quantum limit [Datta (2011)].

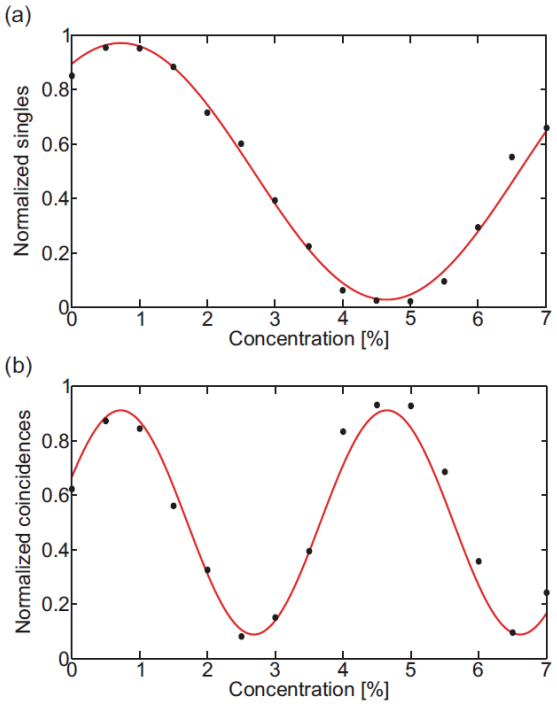

Fig. 6. Quantum interference fringes. Normalized single photon counts (a) and two photon coincidences (b) for different concentrations of bovine serum albumin in a buffer solution (full circles). The solid line represents a fitting of the experimental points with a sinusoidal curve.

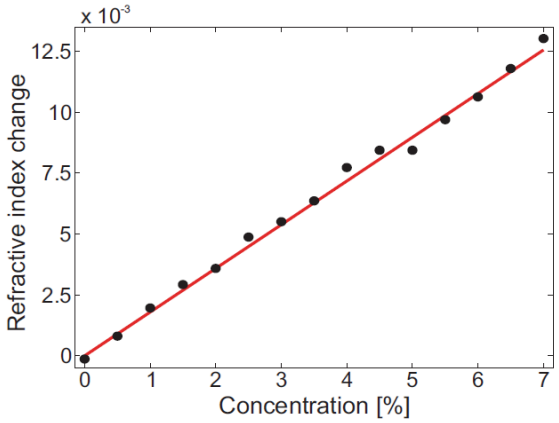

Fig. 7. Refractive index change in the buffer solution as a function of BSA concentration. Experimental data (dots) are shown together with a linear fitting (solid curve).

The refractive index change Δn_S of the BSA solution can be related to the phase shift ϕ, acquired by light during propagation in the sample, which in turn can be estimated from the measured fringes. The dependence of Δn_S on the BSA concentration (Fig. 7) can thus be inferred from the two-photon coincidences reported in Fig. 6(b). The experimental points are well fitted by a linear function, whose slope $dn_S/dC = 1.79\pm0.04\times10^{-3}$ is in very good agreement with the value of 1.82×10^{-3}, previously reported [Barer (1954)] at $\lambda = 0.578$ μm.

4 Conclusions

Monolithic integrated devices allow superior resolution in sensing devices. Single-cell mechanical analysis with optical forces and protein concentration measurement with quantum states of light have been demonstrated in an optofluidic chip. Stability, precise alignment of the components, and simple integration with fluidic circuits make this approach extremely reliable to achieve advanced sensing outside the lab and pave the way to future applications in point-of-care environments.

References

Barer, R., Tkaczyk, S., 1954. Refractive Index of Concentrated Protein Solutions, Nature **173**, 821.

Bellini, N., *et al.*, 2012. Validation and perspectives of a femtosecond laser fabricated monolithic optical stretcher, Biomed. Opt. Express **3**, 2658.

Bragheri, F., *et al.*, 2012. Optofluidic integrated cell sorter fabricated by femtosecond lasers, Lab Chip **12**, 3779.

Corrielli, G., *et al.*, 2013. Fractional Bloch oscillations in photonic lattices, Nature Communications **4**, 1555.

Crespi, A., *et al.*, 2010. Three-dimensional Mach-Zehnder interferometer in a microfluidic chip for spatially-resolved label-free detection, Lab. Chip **10**, 1167.

Crespi, A., *et al.*, 2012. Measuring protein concentration with entangled photons, Appl. Phys. Lett. **100**, 233704.

Datta, A., *et al.*, 2011. Quantum metrology with imperfect states and detectors, Phys. Rev. A **83**, 063836.

de Souza, N., 2012. Single-cell methods, Nat. Methods **9**, 35.

Della Valle, G., Osellame, R., Laporta, P., 2009. Micromachining of photonic devices by femtosecond laser pulses, J. Opt. A: Pure Appl. Opt. **11**, 013001.

Gattass, R. R., Mazur, E., 2008. Femtosecond laser micromachining in transparent materials, Nature Photon. **2**, 219.

Giovannetti, V., Lloyd, S., Maccone, L., 2004. Quantum-Enhanced Measurements: Beating the Standard Quantum Limit, Science **306**, 1330.

Goda, K., *et al.*, 2008. A quantum-enhanced prototype gravitational-wave detector, Nat. Phys. **4**, 472.

Guck, J., *et al.*, 2001. The Optical Stretcher: A Novel Laser Tool to Micromanipulate Cells, Biophys. J. **81**, 767.

Martinez Vazquez, R., *et al.*, 2009. Integration of femtosecond laser written optical waveguides in a lab-on-chip, Lab Chip **9**, 91.

Mitchell, M. W., Lundeen, J. S., Steinberg, A. M., 2004. Super-resolving phase measurements with a multiphoton entangled state, Nature **429**, 161.

Nagata, T., *et al.*, 2007. Beating the Standard Quantum Limit with Four-Entangled Photons, Science **316**, 726.

Osellame, R., *et al.*, 2007. Integration of optical waveguides and microfluidic channels both fabricated by femtosecond laser irradiation, Appl. Phys. Lett. **90**, 231118.

Osellame, R., *et al*., 2011. Femtosecond laser microstructuring: an enabling tool for optofluidic lab-on-chips, Laser Photonics Rev. **5**, 442.

Politi, A., *et al*., 2008. Silica-on-Silicon Waveguide Quantum Circuits, Science **320**, 646.

Peters, T., *The Plasma Proteins* (Academic, 1975).

Rarity, J. G., *et al*., 1990. Two-photon interference in a Mach-Zehnder interferometer, Phys. Rev. Lett. **65**, 1348.

Resch, K. J., *et al*., 2007. Time-Reversal and Super-Resolving Phase Measurements, Phys. Rev. Lett. **98**, 223601.

Sansoni, L., *et al*., 2010. Polarization Entangled State Measurement on a Chip, Phys. Rev. Lett. **105**, 200503.

Sansoni, L., *et al*., 2012. Two-particle bosonic-fermionic quantum walk via integrated photonics, Phys. Rev. Lett. **108**, 010502.

Walther, P., *et al*., 2004. De Broglie wavelength of a non-local four-photon state, Nature **429**, 158.

Whitesides, G. M., 2006. The origins and the future of microfluidics, Nature **442**, 368.